Water distribution within immersed polymer films[§]

Bryan D. Vogt[*a], Christopher L. Soles[a], Vivek M. Prabhu[a], Sushil K. Satija[b], Eric K. Lin[a], Wen-li Wu[a]
[a]Polymers Division, National Institute of Standards and Technology, Gaithersburg, MD
[b]Center for Neutron Research, National Institute of Standards and Technology, Gaithersburg, MD

ABSTRACT

The emergence of immersion lithography for the extension of current lithography tools requires a fundamental understanding of the interactions between the photoresist and the immersion liquid such as water. Neutron reflectometry was used to measure the water concentration depth profile within immersed photoresist films. The bulk of the films swelled to the equilibrium water concentration. However a gradient in water concentration was observed near the polymer/substrate interface. Dependent on the relative hydrophilicity of the polymer and the substrate, either a depletion or excess of water was observed at the interface. Using HMDS treated silicon wafers as the substrate results in approximately 17 % water by volume at the interface. The interfacial concentration decreases (or increases) to the bulk water solubility limit approximately 40 Å from the substrate. As the total film thickness approaches this length scale, the substrate induced concentration gradients lead to a film thickness dependent swelling; enhanced or suppressed swelling is witnessed for the excess or depleted interfacial concentrations, respectively. Variation of the substrate surface energy allows for tuning of the interfacial water concentration, ranging from 30 % to less than 1 % water by volume.

Keywords: photolithography, immersion lithography, thin films

INTRODUCTION

Immersion lithography has emerged as a viable alternative to enhance resolution at future technology nodes, but has lead to several new technical considerations.[1, 2] There has been substantial efforts in identification of immersion fluids,[3] accurate determination of refractive index,[4] and in determining feasibility.[1, 5-7] Currently, immersion lithography utilizing 193 nm radiation is well developed, where water has been identified as one of the leading candidates for the immersion fluid.[6] However, issues that have been neglected in traditional photolithography, such as depth of focus in multilayered media,[8] must be considered in immersion lithography. Additionally, understanding the interactions of water with the photoresist is important to realize the technical feasibility of immersion lithography. Resist swelling can affect resist performance. Water is known to influence the deprotection reaction.[9, 10] However, bulk swelling may not sufficiently explain why certain resist systems fail. Interfacial effects, such as T-topping, footing, and undercutting, commonly have been shown to interfere with the production of high quality features. Variations of water content throughout the film could lead to loss of resolution. Additionally, moisture has been found to be a destabilizing agent to adhesion.[11] The accumulation of water at the buried interface during the immersion process could lead to photoresist delamination. In all these cases, information about the interfacial distribution of water within a thin polymer resist is needed to evaluate and understand its effect on lithographic performance.

Smaller feature dimensions also necessitate decreases in the total film thickness of the photoresist. This is due to design criteria for a maximum aspect ratio, height-to-width on the order of 3:1, beyond which buckling instabilities upon rinsing can lead to pattern collapse. This pattern collapse problem dictates that the film thickness must decrease proportionally to the minimum feature widths. Likewise, smaller features necessitate a shift to shorter wavelength UV radiation, for instance from 248 nm to 193 nm and 157 nm. This is problematic because most polymers strongly absorb at these wavelengths. Thinner resist films designed with optically transparent functional groups reduces UV absorption and ensures illumination throughout the film. With critical dimensions reaching the sub-100 nm mark for chemically

---

[§] Official contribution of the National Institute of Standards and Technology; not subject to copyright in the United States
[*] bryan.vogt@nist.gov

0277-786X/05/$15 · doi: 10.1117/12.599746

amplified photoresist, the influence of the unperturbed dimensions of the polymers that comprise the resist, confinement, and interfacial issues must be considered. It is well known that thin film confinement of a polymer affects several basic thermo-physical properties.[12-14] Additionally, as films become thinner, the fraction of the film that is near the interfaces increases; thus, interfacial phenomenon such as segregation of components is an important consideration for lithography in thin films.[15, 16]

Here we measure the distribution of water within model photoresist films and the influence of surface chemistry on the distribution. The water distribution can be directly quantified using isotopic labeling (D_2O) and neutron reflectivity. However, neutron reflectivity is not required to identify the excess or depletion of water near the substrate. We use a series of x-ray reflectivity measurements over different film thickness to show that for ultrathin films (< 500 Å) there is a thickness dependence on the swelling if the water distribution is non-uniform. Similar measurements could be performed using ellipsometry to identify excess or depletion of water near interfaces.

EXPERIMENTAL METHODOLOGY

1. Materials

This study uses model 248 nm resists: poly(4-tert-butoxycarbonyloxystyrene) (PBOCSt) and poly(4-hydroxystyrene) (PHOSt). While this resist will not likely to be utilized for sub-100 nm lithography because of transparency limitations, it provides a model system for demonstrating general thin film deviations and has been the subject of numerous studies for bulk and thin film effects in the dry state. The PHOSt (Mn,r = 8,000 g mol^{-1}) was purchased from Triquest,[17] while PBOCSt was protected with a tert-butoxycabonyl group (t-BOC) using routes described elsewhere.[18] The chemical structures are identified in Figure 1.

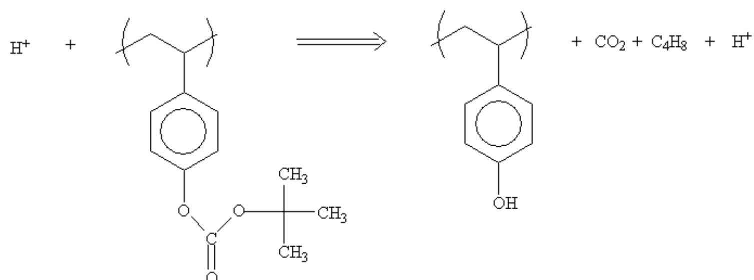

Figure 1. Simplified reaction schematics depicting how a photoacid (H+) reacts with the protected PBOCSt to yield the deprotected and base soluble PHOSt. The photoacid is regenerated by the reaction in addition to evolution of gaseous carbon dioxide and isobutylene.

Either PBOCSt or PHOSt were dissolved in propylene glycol methyl ether acetate (PGMEA) at different mass loadings. The solutions were filtered through a 0.45 µm PTFE filter and spun cast at 209 rad/s (2000 rpm) onto silicon substrates. Different substrate surfaces were examined for their influence on the water distribution profile. For an extremely hydrophilic surface, silicon substrates were pre-treated with UV ozone (UVO), creating a surface that water readily wets. A more hydrophobic surface was created by exposure to hexamethyldisilazane (HMDS) vapor at 120 °C for 5 min. The contact angle was 69° ± 4° for the HMDS treated surface. Additional surfaces were examined with alumina sputtered on the silicon wafer, which has a contact angle of 59.7° ± 1°. This alumina surface could be further treated with either phenylphosphonic acid or n-octyltrichlorosilane, resulting in contact angles of 76.3° ± 1° and 97.3° ± 5° respectively. Each sample, spun coat from different mass fractions to achieve variable film thickness, was post-apply baked 120 °C for 2 h under a vacuum of 0.1 Pa. We have confirmed that these conditions do not induce significant thermal deprotection.

2. Methods

The neutron reflectivity measurements were performed on the NIST Center for Neutron Research (NCNR) NG-7 reflectometer using a wavelength (λ) = 4.768 Å and wavelength spread ($\Delta\lambda/\lambda$) = 0.2. Neutron reflectivity is capable of

probing the neutron scattering length density at depths of up to several thousand Å, with Å depth resolution. All reflectivity measurements were performed at 25 °C for dry films, films equilibrated with saturated deuterium oxide (D_2O) vapor, or films immersed in liquid D_2O. To ensure equilibration, films were exposed to moisture for greater than 4 h. The water distribution vertically through the film can be observed using neutron reflectivity because of the large difference in scattering length density between deuterium and protonated polymers. The immersion experiments utilize an inverted geometry. The neutron beam is incident through the thick silicon wafer and reflected off the thin polymer film. This inverted geometry is used because Si is transparent to the neutrons in comparison to the D_2O. In this inverted geometry on the HMDS treated Si, the films were stable for more than 12 h, without signs of moisture-induced delamination. However, the silicon oxide supported film delaminated quickly in the liquid D_2O precluding any neutron reflectivity measurements. For saturated vapor experiments, the reflectivity geometry was inverted such that the incident beam passed through the vapor phase (or air) before reflecting off the thin polymer film; this is because D_2O saturated vapor is more transparent to the neutrons than solid Si. Additional saturated vapor studies were performed on the alumina and modified alumina surfaces to understand the influence of surface treatment. Whether the incident neutrons first pass through the Si or the vapor is inconsequential in terms of extracting the D_2O absorption profiles in the thin polymer films. The film thickness for both dry and vapor-exposed films was independently corroborated by specular x-ray reflectivity incident through the air/vapor phase; similar measurements are not feasible on the immersed films because both the liquid D_2O and the Si are not transparent to x-rays. The data throughout the manuscript and the figures are presented along with the standard uncertainty (±) involved in the measurement based on one standard deviation. For concentration and thickness determinations, the standard deviation is based upon the goodness of typical fits to the reflectivity data.

RESULTS AND DISCUSSION

In order to quantify the influence of immersion on the water distribution in thin films, the dry state was compared with the immersed state. A typical neutron reflectivity result is shown in Figure 2, for a PBOCSt film on HMDS treated wafer with initial thickness of 535 Å for both the dry and immersed in D_2O case. The reflectivity is shown as a function of the momentum transfer vector, $Q = 4\pi /\lambda \sin(\theta)$. The reflectivity results from the interference of reflected neutrons between the substrate and film and provides detailed information with respect to the neutron scattering length density profile. This profile is modeled by a series of slabs with varying neutron scattering length density and absorbance coefficients. These density profiles are presented in units of Q_c^2 as a function of distance (Z) through the film. Q_c^2 is a scattering length density, with dimensions $Å^{-2}$, and is proportional to the average atomic scattering length, b ($Q_c^2 = 16 \pi Nb$), where N is the number of nuclei. The scattering length density profile for the PBOCSt film illustrates several of the film properties that can be extracted from the reflectivity profile. First, the thickness of the film in the dry and immersed state can be determined. For the PBOCSt on HMDS illustrated here, the film swells from an initial thickness of 535 Å to 543 Å. The scattering length density of each of the layers can also be determined. From the silicon substrate, there are three distinct layers in both the dry and immersed state. First, the oxide layer (near Z = 0 Å) on the silicon that remains unchanged by the immersion. The average Q_c^2 of the polymer film (beyond Z = 0 Å out to approximately Z = 535 Å) increases slightly upon immersion due to the large Q_c^2 of pure D_2O; this is seen by the high Q_c^2 plateau in the immersed profile (solid line). However, the increase in Q_c^2 is not constant across the film as an increase in scattering length density near the HMDS treated silicon oxide surface is observed. This can be attributed to an excess of D_2O at the interface. The maximum D_2O concentration is 17 % by volume at the solid interface and this decays smoothly to the bulk value within 40 Å from the interface. This is significantly greater than the concentration expected from the total film swelling (1.5 % by volume).

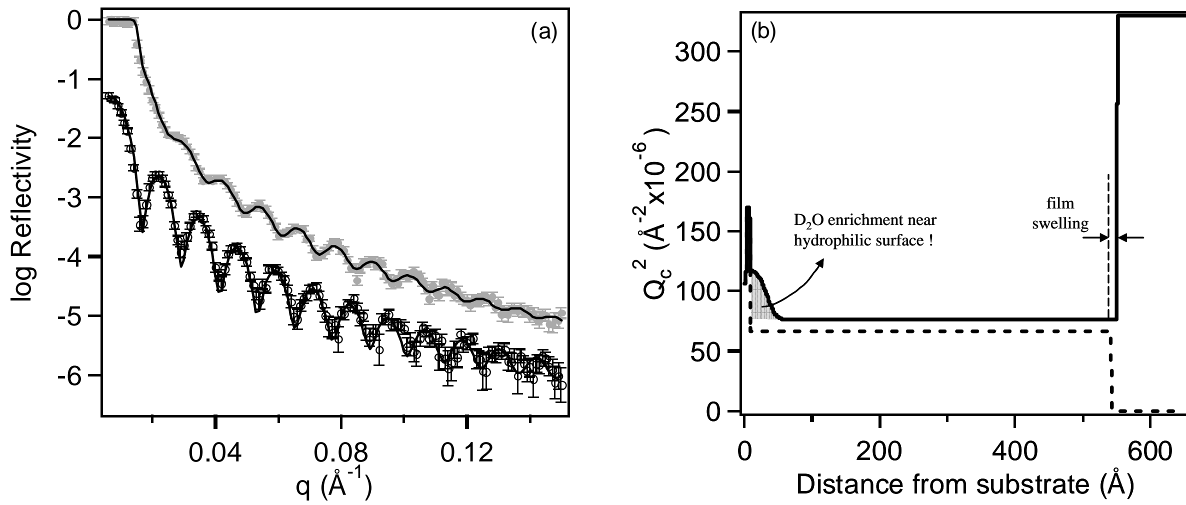

Figure 2. Neutron reflectivity and corresponding fit for initially 535 Å thick PBOCSt film before and after immersion in D_2O. (a) Reflectivity profiles in the dry (open symbols) and immersed (closed gray symbols). The line through the data corresponds to the best fit. The scattering length density profile from the reflectivity fits is shown in (b) for both the dry (dashed line) and immersed (solid line) cases. The region of enhanced D_2O concentration at the silicon oxide interface is shown by the hatched pattern.

The water distribution within PHOSt was also measured in the dry and immersed states on HMDS treated wafers. The reflectivity profiles and corresponding scattering length density profiles for an initially 295 Å thick PHOSt film are shown in Figure 3. Similar to the PBOCSt results, a total film thickness increases due to the absorption of D_2O was observed as the film swelled to 386 Å. A greater extent of swelling is observed, as expected due to the presence of the more hydrophilic hydroxyl groups.

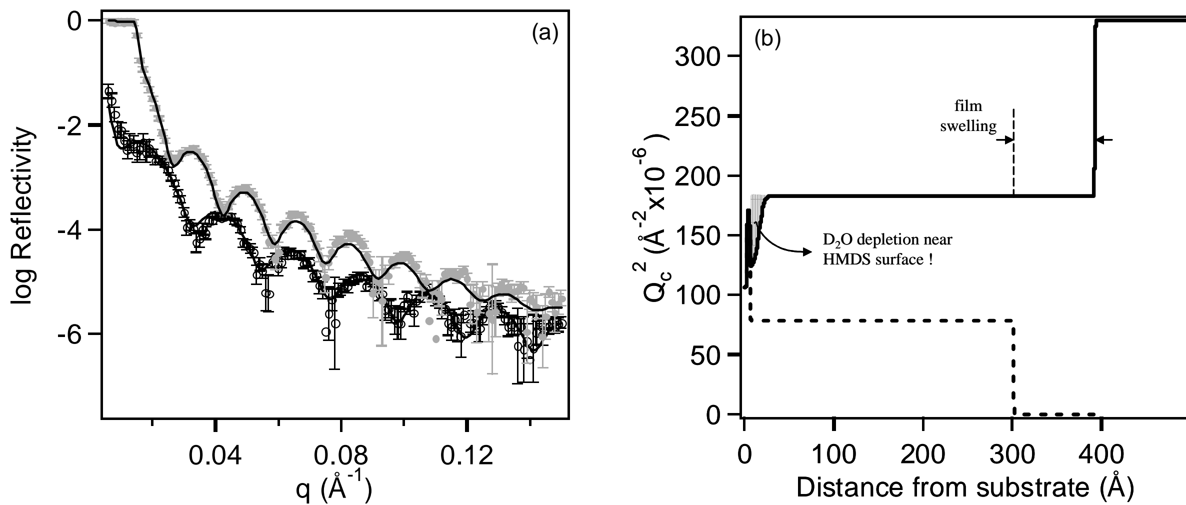

Figure 3. Neutron reflectivity and corresponding fit for initially 295 Å thick PHOSt film before and after immersion in D_2O. (a) Reflectivity profiles in the dry (open symbols) and immersed (closed gray symbols). The line through the data corresponds to the best fit. The scattering length density profile from the reflectivity fits is shown in (b) for both the dry (dashed line) and immersed (solid line) cases. The D_2O depleted region is indicated by the hatched pattern.

One consequence of the increased swelling in the PHOSt is the greater increase in the scattering length density of the film (compare Figs. 2b and 3b). However, the more significant increase in Q_c^2 for the PHOSt is not only due to greater absorption of D_2O, but also to the exchange of hydroxyl protons with deuterium. This proton exchange complicates quantifying the exact water concentration through the film. The largest complication occurs from the decrease in scattering length density near the HMDS surface. This indicates a depletion of water, but the lack of water also limits the proton exchange. Regardless, it is clear that for PHOSt immersed in D_2O on an HMDS treated substrate there is a depletion of water near the substrate, whereas for PBOCSt under the same condition there is an excess of water near the substrate. From this data alone, the determining factor for excess or depletion cannot be distinguished.

In order to understand the cause of the non-uniform water distribution near interfaces, measurements were performed on both PHOSt and PBOCSt on silicon wafers with a more hydrophilic silicon oxide surface. One problem encountered with this system was delamination of the film during the immersed measurement. To circumvent this problem, the films were exposed to saturated D_2O vapor. The use of vapor rather than liquid should not significantly influence the results because the chemical potentials of the saturated vapor and liquid (assuming saturated) are equal. However, the absorption process from the vapor state first requires an adsorption at the free interface that is not necessary in the immersed case, which may lead to differences. Although the absolute concentrations may change, the trends observed from the equilibrated vapor state should be representative of the immersed state.

Neutron reflectivity was again used to measure the water concentration profiles through the film. Using a simple rule of mixtures for the scattering length densities based upon the pure polymer and D_2O scattering length densities, a water concentration profile can be determined. The depth profile of water through PHOSt and PBOCSt films are shown in Figure 4. The PHOSt concentration is calculated assuming all the labile hydroxyl protons are exchanged (this is the minimum concentration). As can clearly be seen, the water concentration near the silicon oxide interface is independent of polymer despite the nearly order of magnitude difference in solubility between PHOSt and PBOCSt. A concentration maximum of roughly 30 % by volume is observed at the interface for both films. This value is consistent with recent results of Kent and coworkers for the water concentration at a silicon oxide interface that is covered with a silane.[19] The water concentration profile in the immersed PBOCSt on HMDS prepared silicon is also shown in Figure 4. This indicates that the moisture concentration at the interface can be tuned by controlling the surface chemistry, whereas a change in the polymer itself does not appear to significantly alter the interfacial water concentration.

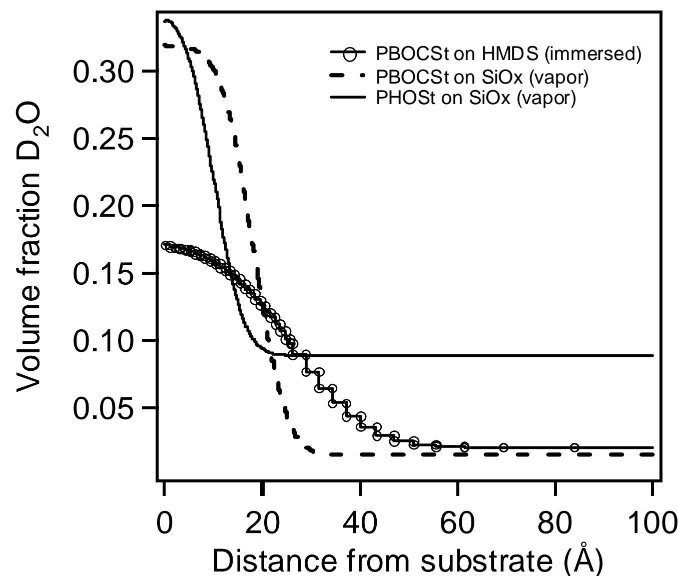

Figure 4. Concentration profiles near the silicon substrate obtained directly from neutron reflectivity measurements similar to those shown in Figs 2 and 3 (reflectivity curves not shown here). The volume fraction of D_2O is determined from the critical angle of the two pure components (polymer and D_2O) using a simple rule of mixtures.

The water concentration profiles near the buried PBOCSt interface was measured in saturated vapor for each of the following substrate treatments: SiO_x, Al_2O_3, HMDS-treated SiO_x, phenylphosphonic acid-treated Al_2O_3, and n-octyltrichlorosilane-treated Al_2O_3. The maximum water concentration for each treatment is shown in Figure 5 as a function of water contact angle. As the substrate becomes more hydrophobic, less water accumulates at the buried interface.

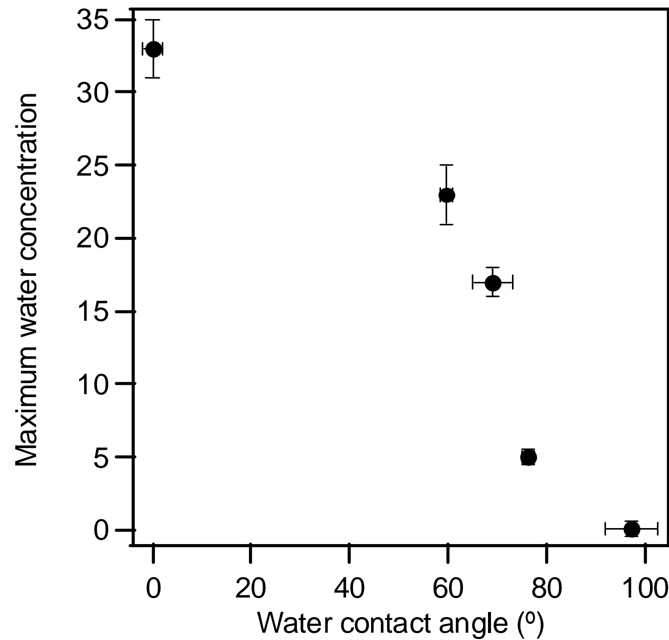

Figure 5. Maximum water concentration near buried PBOCSt/substrate interface for different substrate surface treatments. There is a significant decrease in the water concentration when the substrate water contact angle increases from 60° to 80°.

The amount of water present at the interface rapidly decreases for substrates with water contact angles between 60° and 80°. Through the neutron reflectivity studies, the water concentration at the buried interface can be directly measured. However, the amount of water at the interface can be inferred through indirect means by measuring the swelling as a function of film thickness for ultrathin films. Figure 6 shows the film thickness dependent swelling of PBOCSt on Al_2O_3 and SiO_x surfaces. Since more water accumulates at the PBOCSt/SiO_x interface than PBOCSt/Al_2O_3 interface, the thin films on SiO_x swell significantly more than on Al_2O_3. The film thickness was measured using x-ray reflectivity, where there is minimal contrast between the PBOCSt and H_2O, in dry (h_0) and wet (h) states. Due to the limited contrast, only information on the film swelling was obtained. However using the film thickness dependence of the swelling, the conclusions from the direct measurement of the water profile using NR can be inferred.

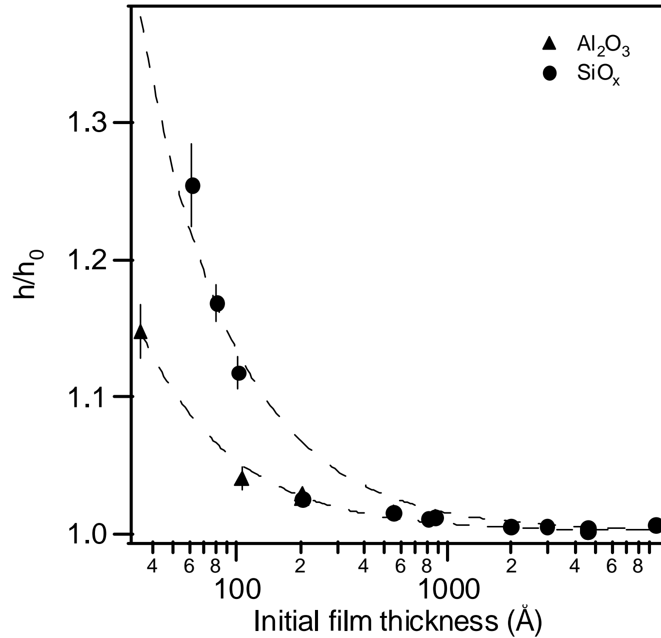

Figure 6. Film thickness dependent swelling of PBOCSt in saturated H_2O vapor when supported on silicon wafer with either Al_2O_3 or SiO_x surfaces.

The thickness dependent swelling was found to be well represented by a zero-adjustable parameter model, consisting of an excess layer at the polymer / substrate interface and bulk swelling of the polymer. The extent of swelling (h/h_0) can be written as:

$$\frac{h}{h_0} = 1 + \frac{\Delta h_{eq} + h_{excess}}{h_i}$$

where h is the swollen film thickness, h_0 is the initial film thickness, Δh_{eq} is the thickness change from bulk swelling, and h_{excess} is the equivalent water thickness corresponding to the accumulation at the interface. From the x-ray reflectivity measurements, both h and h_0 are determined, but h can be predicted from h_0 if the equilibrium swelling and excess are known. h_{excess} can be determined from integration of the excess water from one neutron reflectivity experiment such as that shown in Figure 2. This integration is represented by the area under the total D_2O concentration curve (see Figure 4). There is significantly less total water accumulation at the Al_2O_3 interface in comparison to the SiO_x interface. This is responsible for the difference in the swelling in the thin PBOCSt films. The fit of the data to this model is shown by the dashed lines in Figure 6. There is good agreement between the predictions from this simple model and the experimental results. Similar insight into moisture accumulation for other systems can be obtained from ellipsometric measurements on different film thicknesses.

CONCLUSIONS

The distribution of deuterium oxide within model photoresist films has been probed directly using neutron reflectivity. There is a region near the buried interface where the water concentration deviates from the bulk. Both an increase and decrease in relative concentration has been observed depending upon the polymer and substrate. For PHOSt and PBOCSt supported on silicon oxide surface substrate, there was an excess of water at the interface observed with a maximum concentration of approximately 30 % by volume in both cases for saturated D_2O vapor equilibration. For immersed PBOCSt supported on HMDS-treated silicon wafer, an excess concentration was observed as well, but the maximum concentration at the interface was only 17 % by volume. The depletion of water was observed for PHOSt on HMDS treated wafers for the D_2O immersion experiment. For the PBOCSt, additional surfaces were examined to

determine the surface required for no water accumulation. There is a significant drop in the water concentration at the buried interface when the water contact angle of the surface increases from 60° to 80°. Thus, the absolute interfacial concentration is highly dependent upon the chemistry of the supporting surface, but does not appear strongly dependent upon the photoresist itself. The excess water at the interface also manifests itself as a thickness dependent swelling for thin films, allowing for observation of interfacial concentration heterogeneities in the laboratory without the use of neutrons.

ACKNOWLEDGEMENTS

Funding for this work comes in part from the DARPA Advanced Lithography Program, grant N66001-00-C-8083 and the NIST Office of Microelectronics Programs Support for Bryan Vogt comes from the National Research Council NIST Postdoctoral Fellowship Program. The authors thank Young-Soo Seo for assistance with neutron reflectivity measurements.

REFERENCES

1. Lin BJ. Immersion lithography and its impact on semiconductor manufacturing. Journal of Microlithography Microfabrication and Microsystems 2004; 3(3):377-395.

2. Switkes M, Kunz RR, Rothschild M, Sinta RF, Yeung M, Baek SY. Extending optics to 50 nm and beyond with immersion lithography. Journal of Vacuum Science & Technology B 2003; 21(6):2794-2799.

3. Switkes M, Rothschild M. Immersion lithography at 157 nm. Journal of Vacuum Science & Technology B 2001; 19(6):2353-2356.

4. Burnett JH, Kaplan SG. Measurement of the refractive index and thermo-optic coefficient of water near 193 nm. Journal of Microlithography Microfabrication and Microsystems 2004; 3(1):68-72.

5. Dammel RR, Houlihan FM, Sakamuri R, Rentkiewicz D, Romano A. 193 nm immersion lithography - Taking the plunge. Journal of Photopolymer Science and Technology 2004; 17(4):587-601.

6. Owa S, Nagasaka H. Advantage and feasibility of immersion lithography. Journal of Microlithography Microfabrication and Microsystems 2004; 3(1):97-103.

7. Mulkens J, Flagello D, Streefkerk B, Graeupner P. Benefits and limitations of immersion lithography. Journal of Microlithography Microfabrication and Microsystems 2004; 3(1):104-114.

8. Lin BJ. Depth of focus in multilayered media - a long-neglected phenomenon aroused by immersion lithography. Journal of Microlithography Microfabrication and Microsystems 2004; 3(1):21-27.

9. Bruce JA, Dupuis SR, Gleason R, Linde H. Effect of Humidity on Photoresist Performance. J Electrochem Soc 1997; 144(9):3169-3174.

10. Burns SD, Medeiros DR, Johnson HF, Wallraff GA, Hinsberg WD, Willson CG. The effect of humidity on hte deprotection kinetics of chemically amplified resists. Proceedings of the SPIE: Advances in Resist Technology and Processing XIX 2002; 4690:321-331.

11. Kinloch AJ. Adhesion and Adhesives Science and Technology. London: Chapman and Hall, 1987.

12. Goldfarb DL, Angelopoulos M, Lin EK, Jones RL, Soles CL, Lenhart JL, Wu WL. Confinement effects on the spatial extent of the reaction front in ultrathin chemically amplified photoresists. Journal of Vacuum Science & Technology B 2001; 19(6):2699-2704.

13. Soles CL, Lin EK, Lenhart JL, Jones RL, Wu WL, Goldfarb DL, Angelopoulos M. Thin film confinement effects on the thermal properties of model photoresist polymers. Journal of Vacuum Science & Technology B 2001; 19(6):2690-2693.

14. Soles CL, Douglas JF, Lin EK, Lenhart JL, Jones RL, Wu WL, Goldfarb DL, Angelopoulos M. Incoherent neutron scattering and the dynamics of thin film photoresist polymers. Journal of Applied Physics 2003; 93(4):1978-1986.

15. Jablonski EL, Sambasivan S, Lin EK, Fischer DA, Devadoss C, Puligadda R. Near edge x-ray absorption fine structure measurements of the interface between bottom antireflective coatings and a model deprotected photoresist. Journal of Vacuum Science & Technology B 2003; 21(6):3153-3156.

16. Jablonski EL, Prabhu VM, Sambasivan S, Lin EK, Fischer DA, Goldfarb DL, Angelopoulos M, Ito H. Near edge x-ray absorption fine structure measurements of surface segregation in 157 nm photoresist blends. Journal of Vacuum Science & Technology B 2003; 21(6):3162-3165.

17. Certain commercial equipment and materials are identified in this paper in order to specify adequately the experimental procedure. In no case does such identification imply recommendations by the National Institute of Standards and Technology nor does it imply that the material or equipment identified is necessarily the best available for this purpose.

18. Frechet JM, Eichler E, Ito H, Willson CG. Poly(para-tert-butoxycarbonyloxystyrene) - A convenient precursor to para-hydroxystyrene resins. Polymer 1983; 24(8):995-1000.

19. Kent MS, Smith GS, Baker SM, Nyitray A, Browning J, Moore G. The effect of a silane coupling agent on water adsorption at a metal/polymer interface studied by neutron reflectivity and angle-resolved X-ray photoelectron spectroscopy. Journal of Materials Science 1996; 31:927-937.